P-T-t trajectory of metamorphic rocks from the central Chiapas Massif Complex: the Custepec Unit, Chiapas, Mexico

Juliana Estrada-Carmona[1,*], Bodo Weber[1], Lutz Hecht[2], Uwe Martens[3]

[1] División Ciencias de la Tierra, Centro de Investigación Científica y de Educación Superior de Ensenada (CICESE), Carretera Tijuana-Ensenada Km. 107, 22860 Ensenada B.C., Mexico.
[2] Leibniz-Institut für Evolutions- und Biodiversitätsforschung, Humboldt-Universität Berlin, Invalidenstrasse 43, D-10115, Berlin,Germany.
[3] Department of Geological and Environmental Sciences, Stanford University, 450 Serra Mall, Braun Hall, Building 320, Stanford, CA 94305-2115, USA.
** jestrada@cicese.mx*

ABSTRACT

The Chiapas Massif, located in the southwestern Maya terrane, is primarily composed of igneous and metaigneous rocks of Late Permian - early Triassic age, although two distinct metasedimentary units have also been recognized. The Sepultura Unit, located in the nothwestern Chiapas Massif, is composed of psammites, pelites and calcsilicate rocks metamorphosed under high-T, low- to medium-P conditions. The Custepec Unit, which is the object of this study, is located in the central-southeastern portion of the Chiapas Massif and is composed of partially melted amphibolites interbedded with quartzofeldspathic and pelitic gneisses, marbles, calcsilicate rocks, and quartzites. Geothermobarometry of a metapelite and an amphibolite yielded consistent metamorphic conditions of ~800 ºC and 9 kbar. These pressure and temperature estimates, along with petrographic observations indicate that metamorphic conditions were in the amphibolite-granulite facies transition at ~25–30 km depth. A Sm-Nd garnet-whole rock age of 268 ± 9 Ma, which predates a previously published U-Pb zircon age of anatectic and metamorphic zircons of 252 ± 4 Ma, indicates that Sm and Nd in garnet behaved as a closed system during high-grade metamorphism, while zircon crystallized at temperatures below the metamorphic peak. The high-grade metamorphic event was followed by a phase of isobaric cooling, medium grade retrogression reactions, uplift and greenschist facies diaphtoresis accompanied by further ductile deformation.

Key words: metamorphism, geothermobarometry, metapelite, garnet-amphibolite, Custepec, Chiapas Massif, Maya block, Mexico.

RESUMEN

El Macizo de Chiapas está localizado en el sur del terreno Maya y está compuesto, en su mayoría, por rocas ígneas y metaígneas del Pérmico tardío al Triásico temprano. Se han reconocido dos unidades metasedimentarias: (1) La Unidad La Sepultura, ubicada en el noroeste del macizo, compuesta por samitas, pelitas y rocas calcosilicatadas metamorfizadas bajo condiciones de alta temperatura y baja a media presión; y (2) la Unidad Custepec, que es objeto del presente trabajo, está localizada en el centro-sureste del macizo. Está compuesta principalmente por anfibolitas parcialmente fundidas intercaladas

con gneises cuarzo-feldespáticos y pelíticos, mármoles, rocas calcosilicatadas y cuarcitas. Se utilizó el geotermómetro de intercambio de iones de Fe^{+2}-Mg entre granate y biotita (GARB), y los geobarómetros granate+aluminosilicato+cuarzo+plagioclasa (GASP) y granate+rutilo+alumosilicato+ilmenita+cuarzo (GRAIL) en una metapelita; para calcular las condiciones de metamorfismo de una anfibolita con granate se usó el termómetro hornblenda - plagioclasa y el geobarómetro de granate - plagioclasa - hornblenda - cuarzo. Los resultados son consistentes e indican que el metamorfismo en la Unidad Custepec alcanzó temperaturas de ~800 ºC y presiones de ~9 kbar. Esto, sumado a observaciones petrográficas, permite ubicar el metamorfismo en la facies de anfibolita alta o transición a la facies de granulita en un nivel cortical entre 25 y 30 km. Una edad Sm-Nd en granate – roca total de 268 ± 9 Ma, que antecede a una edad U-Pb en circones previamente publicada de 252 ± 4 Ma, indica que los elementos Sm y Nd en granate se comportaron como un sistema cerrado durante el metamorfismo de alto grado, mientras que el zircón cristalizó a temperaturas por debajo del pico metamórfico. Después del evento metamórfico de alto grado ocurrió una fase de enfriamiento isobárico, reacciones retrógradas de grado medio, levantamiento y retrogresión en facies de esquisto verde acompañada por deformación dúctil.

Palabras clave: metamorfismo de alto grado, geotermobarometría, metapelita, anfibolita de granate, Custepec, Macizo de Chiapas, bloque Maya, México.

INTRODUCTION

The geology of southern Mexico and Central America has been interpreted in terms of a collage of tectonostratigraphic terranes or crustal blocks (Campa and Coney, 1983; Dickinson and Lawton, 2001). Correlations between these crustal blocks and the core of the North American plate remain uncertain. Crustal blocks relevant to the this paper are the Mixteco terrane, the Zapoteco terrane, the Maya and the Chortís blocks (Figure 1). According to Dickinson and Lawton (2001), these crustal blocks reached their current location prior to the Triassic opening of the Gulf of Mexico by large-scale sinistral movements. In order to systematically compare and correlate south Mexican and Central American terranes it is necessary to establish the thermobaric structure and timing of metamorphism of each individual terrane. The metamorphic evolution of the basement of each terrane can conveniently be represented as a pressure-temperature-time (P-T-t) path. Consequently, obtaining P-T-t paths for each terrane is critical for their systematic comparison. P-T-t paths offer valuable constraints to a better understanding of the geologic processes that led to the present configuration of crustal pieces, for instance, the much debated juxtaposition of the Maya and Chortis blocks.

In this contribution we present the results of a MS thesis that was focused on a metamorphic suite of rocks (the Custepec Unit) in the central-southern Chiapas Massif, which is the crystalline basement of the southern Maya block. Besides geologic mapping, petrographic, and structural documentation of the study area, the main goal of this study is to document the metamorphic evolution of the Custepec Unit by presenting geothermobarometric calculations that were obtained from the mineral chemistry of selected metamorphic samples. Geochronologic data from the same area complement our P-T-t path.

GEOLOGICAL SETTING

Regional Geology

Southern Mexico and Central America are composed of several blocks or terranes with differing geologic records and separated by major faults (Sedlock *et al.*, 1993). Pre-Mesozoic basement has been reported in the Mixteco terrane (Paleozoic polymetamorphic Acatlán Complex; *e.g.*, Keppie *et al.*, 2008, and references therein), the Zapoteco terrane with its Grenvillian Oaxacan Complex (Ortega-Gutiérrez, 1981, 1984; Solari *et al.*, 2003), the Chortís block (Manton, 1996), and Maya block (Figure 1).

The Maya block (Dengo,1985), Maya terrane (*e.g.*, Manton, 1996), or Yucatán-Chiapas block (Sedlock *et al.*, 1993) is the southernmost of the Mexican terranes (Figure 1) and geographically encompasses the Yucatán Peninsula, parts of the coastal plains of the Gulf of Mexico, central Guatemala, and southeastern Mexico to the Tehuantepec Isthmus. Pre-Mesozoic rocks of the Maya block are mainly exposed along its southern limit, north of the Polochic fault and within the Chiapas Massif (Figure 1). Further north pre-Mesozoic rocks are known only from the Maya Mountains of Belize (Bateson and Hall, 1977; Steiner and Walker, 1996; Martens *et al.*, 2006) and from the Grenville aged Guichicovi Complex (Weber and Köhler, 1999) at the western edge of the Maya block (Figure 1). The southern limit of the Maya block is related to the Motagua-Polochic fault system, where the North American plate has been truncated during Cenozoic sinistral strike-slip movements (*e.g.*, Burkart, 1983). According to Ortega-Gutiérrez *et al.* (2007) several crustal slices with different metamorphic basement and stratigraphic cover have been distinguished between the Polochic and the Motagua fault, making the definition of the limit between the Maya and the Chortís blocks a challenging question. In central Guatemala, the

Figure 1. a: Plate-tectonic overview and main terranes of southern Mexico and Central America. MPS: Motagua-Polochic System; TMVB: Trans-Mexican-Volcanic Belt; terrenos: Mix: Mixteco; Cha: Chatino; Z: Zapoteco; Cui: Cuicateco. b: Simplified geologic map showing pre-Mesozoic rocks exposed in southeastern Mexico and Central America (modified after Weber *et al.*, 2006). Abbreviations: CM: Chiapas Massif, CHU: Sierra de Chuacús, MM: Maya Mountains.

Chuacús Complex of Devonian to Pennsylvanian age is composed dominantly of metasedimentary rocks that underwent metamorphism and deformation at high pressure and high temperature (Ortega-Gutiérrez *et al.*, 2004; Martens *et al.*, 2007; Solari *et al.*, in press). Ortega- Gutiérrez *et al.* (2004, 2007) proposed that the Chuacús Complex is an independent fault-bounded terrane possibly accreted to the Maya block.

The Chortís block comprises part of Guatemala, Honduras, Nicaragua and Salvador (*e.g.*, Dengo, 1985 and references therein). The basement of the Chortís block is composed of metamorphic rocks of possible Precambrian age (Manton, 1996; Nelson *et al.*, 1997) that include paragneisses and orthogneisses, metasedimantary and metavolcanic rocks, as well as deformed early Mesozoic plutons (Sedlock *et al.*, 1993). The northern limit of the Chortís block is the Motagua fault zone, which includes a mélange containing blocks of ophiolitic nature and metamorphic rocks such as amphibolite, eclogite, albitite and jadeitite that range in age from 78 to 64 Ma north of the Motagua Fault zone and from 125 to 113 Ma south of it (Harlow *et al.*, 2004; Martens *et al.*, 2005). The latter ages were interpreted as the approximate time of the collision between the Chortís block and southern Mexico. The Maastrichtian ages record subduction related to the collision of an extension of the Chortís block, perhaps the Nicaraguan Rise, with the Maya block (Harlow *et al.*, 2004).

The Chiapas Massif

The Chiapas Massif represents the crystalline basement of the southern Maya block (Figure 1). It is the largest Permian-Triassic batholithic structure of Mexico, covering an area of ~20,000 km^2, and is also referred to as the Chiapas Batolith (Morán-Centeno, 1984 and references therein). The

Chiapas Massif was interpreted as being part of a continental arc that formed along the western margin of Mexico in Permian-Triassic times (Torres *et al.*, 1999). Most of the Chiapas Massif is composed of orthogneisses, commonly augen-gneisses, and migmatites, which were interpreted as being of metaigneous origin due to their homogeneity at outcrop scale, their homogeneous chemical and mineralogical composition, and their lack of muscovite, garnet, Al_2SiO_5 polymorphs, garnet, and/or other Al-rich phases like cordierite (Schaaf *et al.*, 2002). Metaigneous rocks from the Chiapas Massif differ from those of other granitoids of similar age in Mexico (Damon *et al.*, 1981; Torres *et al.*, 1999) by their penetrative, mostly E-W striking foliation and their compositional variation ranging from gabbro to granite (Schaaf *et al.*, 2002).

Recent work has revealed that the metaigneous rocks are associated to metasedimentary rocks, which were first described at a locality ~50 km west of Villaflores (Figure 1) and were named the Sepultura Unit (Weber *et al.*, 2002, 2007). The Sepultura Unit is mainly composed of metapsammites and metapelites, with garnet, sillimanite, cordierite and Ti-bitotite-bearing assemblages, intercalated with marble, calcsilicate rocks and metagreywackes. The calcsilicate rocks have two assemblages: 1) garnet, clinopyroxene with or without wollastonite, and 2) feldspar, clinopyroxene, clinozoisite, and quartz. Calcic marbles locally contain olivine or garnet lumps. Garnet-biotite thermometry and garnet + aluminosilicate + quartz + plagioclase (GASP) barometry yielded peak metamorphic conditions of 730–780 ºC and 5.8 kbar with retrograde assemblages that equilibrated at 540 ºC and 4.5 kbar (Hiller *et al.*, 2004).

The Custepec Unit, which crops out in the central part of the southern Chiapas Massif, was defined by Weber *et al.* (2007) as an independent unit because rocks from the Custepec area differ from those of the Sepultura Unit by their protolith composition and metamorphic conditions. The Custepec Unit is characterized by the abundance of mafic gneisses and amphibolites that contain lenses of, or are interlayered with, marbles and calcsilicate rocks. On the basis of these characteristics and the presence of abundant Mesoproterozoic detrital inherited zircon cores in the amphibolites, a volcanosedimentary origin was suggested for the Custepec Unit (Weber *et al.*, 2007). Additionally, mineral assemblages like Ti-rich biotite + garnet + plagioclase + quartz in metapelitic gneisses, the presence of Ti-rich hornblende and anatexis of the amphibolites forming neosomes composed of garnet + plagioclase ± Kfeldspar + quartz + titanite, indicate metamorphic conditions in the amphibolite to granulite-facies transition. The observed assemblage of garnet + hornblende + plagioclase indicates a P-T-path with higher relative pressures compared to the low P-T-path of the Sepultura Unit.

The first reliable geochronologic data were reported by Damon *et al.* (1981), including a Rb-Sr whole rock isochron for 10 granitic rocks with an age of 256 ± 10 Ma. Available geochronologic data for the Chiapas Massif is not conclusive. Torres *et al.* (1999) compiled older K-Ar data ranging from 271 to 239 Ma for different samples from the Chiapas Massif. Rb-Sr ages for mica-whole rock pairs range from 244 ± 12 to 214 ± 11 Ma (Schaaf *et al.*, 2002), indicating cooling in the Triassic. Weber *et al.* (2005) performed U-Pb (ID-TIMS) analysis of zircons from orthogneisses from the Chiapas Massif that yielded lower intercept ages that range from 258 ± 2 to 251 ± 2 Ma, and interpreted the results as dating the age of a major tectonothermal event. Upper concordia intercepts yielded Mesoproterozoic ages. Many orthogneisses, however, have more complex zircons, that resulted in imprecise intercept ages. U-Pb by SHRIMP revealed that ~254 Ma old metamorphic zircon overgrowths document the high-grade metamorphic event that led also to partial anatexis of pelitic and psammitic metasedimentary rocks of the Sepultura Unit (Weber *et al.*, 2007). Zircons that grew during anatexis, and metamorphic overgrowth around preexisting zircons from an amphibolite of the Custepec Unit yielded (within error) an identical age of 252 ± 2.4 Ma. U-Pb SHRIMP data of magmatic zircon zones from an anatectic orthogneiss that yielded a concordia age of 272 ± 3 Ma indicate the time of crystallization of the igneous precursor. The latter age proofs that mid-Permian plutons intruded the Chiapas Massif prior to the Late Permian metamorphic event (Weber *et al.*, 2007). Similar mid-Permian plutonic rocks have been reported from other localities in Mexico and in Guatemala (Damon *et al.*, 1981; Yañez *et al.*, 1991; Solari *et al.*, 2001; Elías-Herrera and Ortega-Gutiérrez, 2002; Ducea *et al.*, 2004).

ANALYTICAL METHODS

Samples were collected to carry out petrography, geochronology, and geothermobarometry. Major element analyses were obtained for garnet, biotite, plagioclase, ilmenite and amphibole. Electron microprobe analyses and back scatter electron images were performed on a Jeol JXA-8800 at the Humboldt Universität, Berlin, a JEOL JXA-8200 at the Freie Universität, Berlin, and a JEOL JXA-733A at Stanford University. Operating conditions for microprobe analyses were 15 kV and 15 nA (Berlin), and 24 nA (Stanford). Analyses were calibrated using Smithsonian international mineral standards. Counting times were 20 s on peak and 10 s on backgrounds. The reproducibility of test measurements on plagioclase and garnet standards was generally much better than 2 % (one sigma), except for values close to the detection limit, where the reproducibility may be reduced to about 10%.

Pressure and temperature conditions were calculated for two suitable samples using *Thermobarometry v 2.1* software by Spear and Kohn (1999). Sample JMC-68b is a garnet-sillimanite-biotite gneiss that was suitable for applying the garnet + aluminosilicate + quartz + plagioclase (GASP) and the garnet + rutile + aluminosilicate + ilmenite + quartz (GRAIL, Bohlen *et al.*, 1983) barometers, and

the Fe^{+2}-Mg exchange Grt-Bt thermometer (GARB). The calibration used for the GRAIL barometer is exactly as presented in Bohlen *et al.* (1983) with the addition of a Ca-Mg garnet correction (following Hodges and Spear, 1982). Sample JMC-01 is a garnet amphibolite suitable for the garnet + plagioclase + hornblende + quartz barometer (Kohn and Spear, 1990). Temperature estimates for this rock were calculated using the hornblende + plagioclase thermometer of Holland and Blundy (1994).

Sample preparation and wet chemical procedure for Sm-Nd isotope analysis was performed according to Weber and López-Martínez (2006). About ~200 mg of garnet was separated from a garnet-amphibolite (CB45). The dissolved garnet sample was split into two aliquots (1/3 and 2/3). The smaller (1/3) aliquot was spiked for isotope dilution analysis (ID-run) for both Sm and Nd; the larger aliquot was used for the Nd isotope composition run, to achieve precise isotopic ratios. Sm and Nd isotopic ratios were measured in static mode on a Finnigan MAT 262 mass spectrometer at the Laboratorio Universitario de Geoquímica Isotópica at Universidad Autónoma de Mexico. Sm and Nd isotopic ratios were corrected for mass fractionation by normalizing to $^{152}Sm/^{147}Sm = 1.78308$ and $^{146}Nd/^{144}Nd = 0.7219$.

GEOLOGY AND PETROGRAPHY OF THE CUSTEPEC UNIT

Geologic mapping was carried out around 'Finca Custepec' at 1:25.000 scale, covering an area of ~40 km^2 (Figure 2). Various rock types, all of which are spatially related, intercalated, or transitional, were identified and

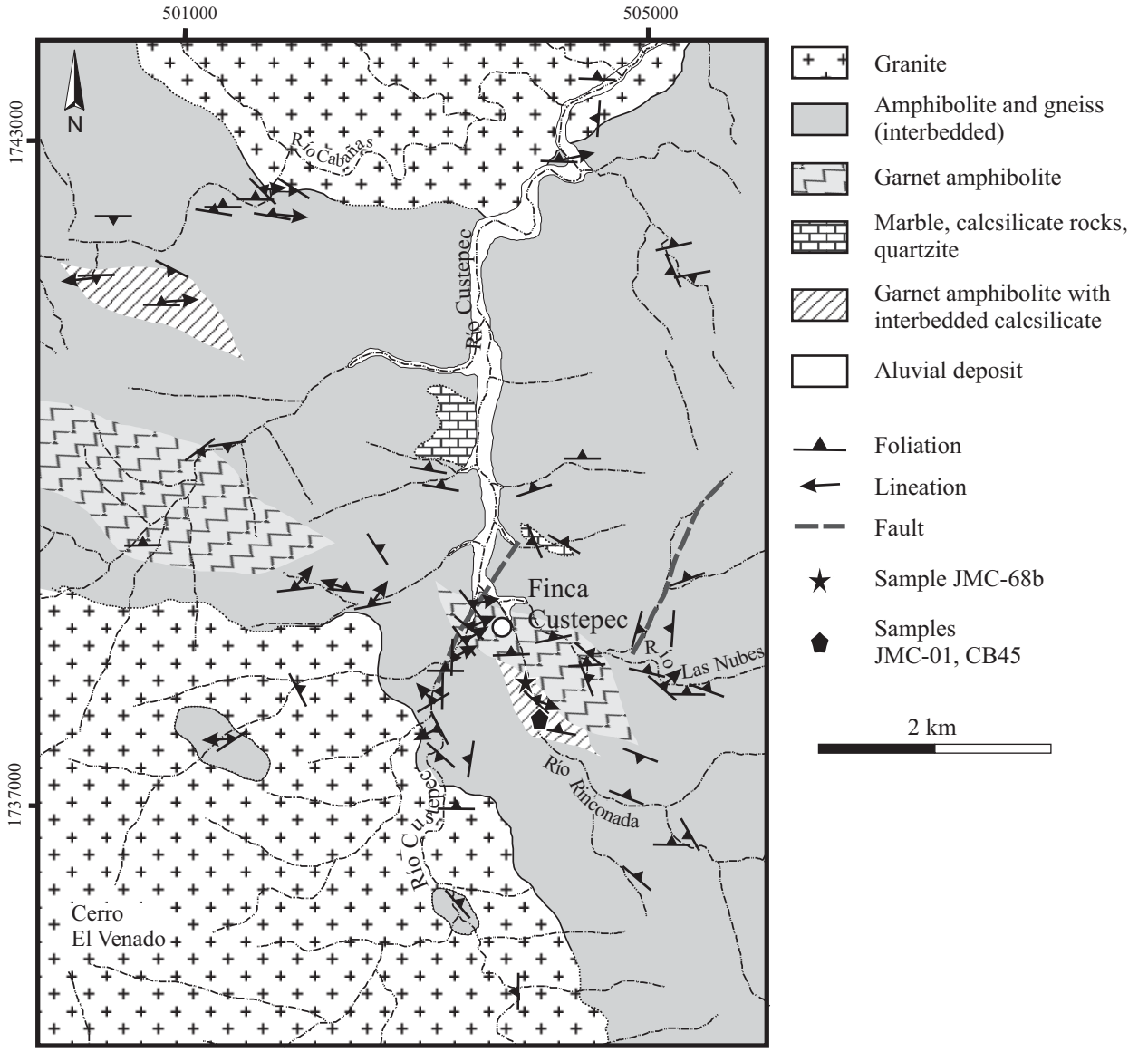

Figure 2. Geological map of the Custepec Unit showing mapped lithologic units, sample locations, and structures.

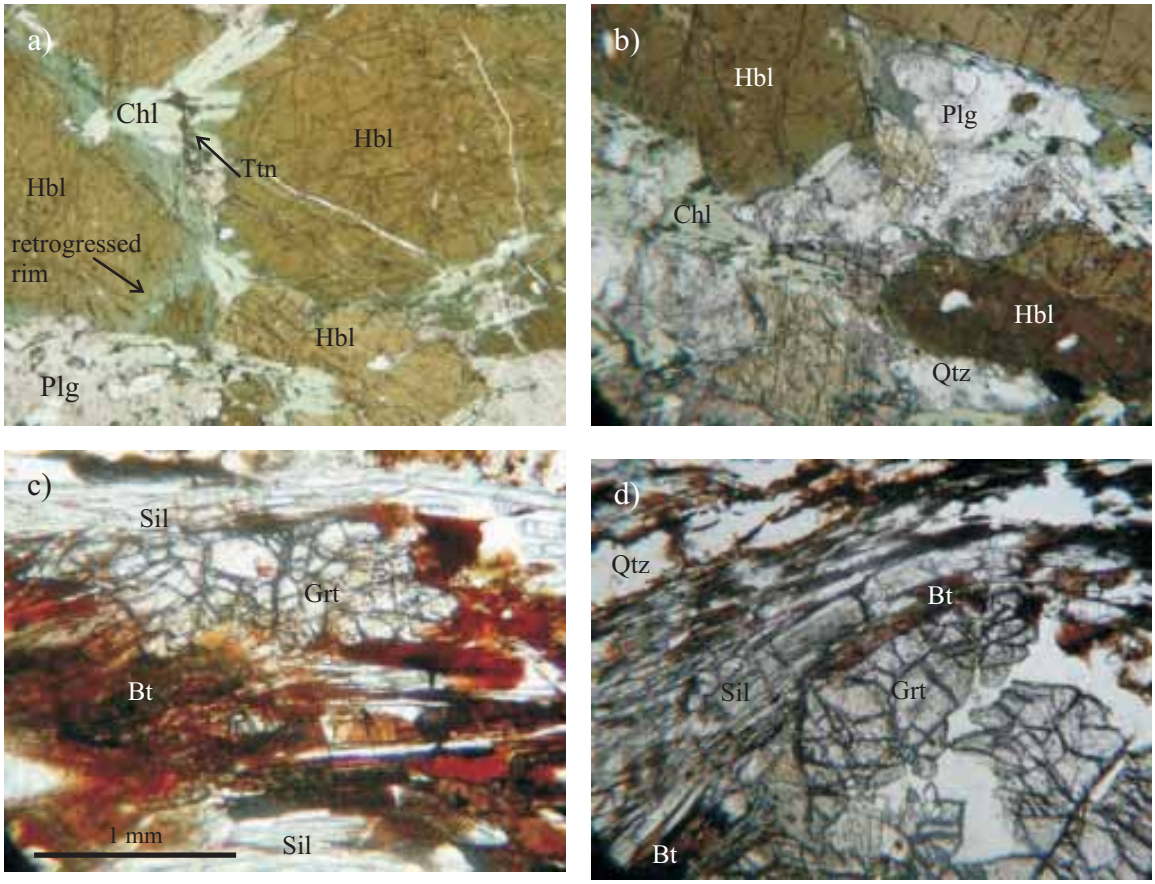

Figure 3. Photomicrographs of garnet amphibolite and metapelite. a: Ti-rich hornblende showing retrograde rims and breakdown to chlorite and titanite (sample JMC-01). b: Hornblende crystals, chlorite as a breakdown product from biotite, partially sericitized plagioclase (sample JMC-01). c and d: Biotite and sillimanite rich domains with coexisting garnet. Bt: biotite; Chl: chlorite; Grt: garnet; Hbl: hornblende; Plg: plagioclase; Qtz: quartz; Sil: sillimanite; Ttn: titanite.

referred to as the Custepec Unit. In the following, the individual lithologies as they are shown on Figure 2 are described in detail.

Amphibolites

Amphibolite is the most prominent rock type of the study area. Two main types of amphibolites were recognized in the Custepec Unit: 1) garnet-bearing amphibolites and 2) garnet-free amphibolites. Ubiquitously, they display abundant compositional layering, best observed at outcrop scale. Garnet-bearing amphibolites are medium grained with gneissic texture. Migmatitic features were observed locally; they are characterized by centimeter to decimeter wide neosomes, which are composed of quartz, plagioclase, and minor garnet. Garnets occur as poikiloblasts up to 3 cm in diameter, containing inclusions of biotite, quartz, and epidote. Garnet also contains numerous fractures filled with secondary chlorite. In some of the samples garnet is surrounded by plagioclase coronas. In most amphibolites, the mineral assemblage is hornblende + plagioclase + quartz ± garnet ± biotite. Hornblende is typically subhedral and contains apatite and titanite inclusions. Occasionally, amphiboles display zoning, having brown cores and green to olive green rims (Figures 3a and 3b). Plagioclase is subhedral and partially sericitized. Quartz is present as smaller anhedral grains and exhibits undulose extinction. Accesory minerals include epidote, opaque minerals, titanite and apatite (see Table 1 for sample mineralogy).

Table 1.Mineralogy of samples from the Custepec Unit, Chiapas Massif Complex.

	Major phases						Minor phases								
Rock type	**Grt**	**Bt**	**Plg**	**Qtz**	**Sil**	**Am**	**Zrn**	**Opq**	**Ap**	**Ep**	**Rt**	**Ttn**	**Chl**	**Kfs**	**White mica**
Pelitic gneiss	x	x	x	x	x		x	x	x		x		bp	x	bp
Garnet amphibolite	x	x	x	x		x	x	x	x	bp		x	bp		

bp, mineral present only as breakdown product.

Gneisses

Three types of gneisses are distinguished in the Custepec Unit:

1) Sillimanite+garnet-bearing biotite gneiss is exposed only in the Rinconada river (Sample JMC-68b, Figure 2), approximately 500 m from Finca Custepec, but many cobbles were found along the Custepec river. The paragneiss is medium grained and is interlayered with garnet-bearing amphibolites. The paragneiss displays ubiquitous compositional layering with sillimanite- and biotite-rich domains, which contain minor garnet (Figure 3c and d), and quartzofeldspathic domains with garnet. The former domains contain the assemblage biotite + garnet + sillimanite + plagioclase + quartz + K-feldspar and, therefore, we interpret this sample as a metapelite. Biotite is dark brown with a reddish tint. Large (2–3 mm), euhedral sillimanite crystals and biotite have a preferred orientation defining the foliation. Sillimanite is partly altered to fine grained white mica. Garnet is anhedral and poikiloblastic, ranging in size from 2 mm to 1 cm, with quartz, biotite, ilmenite, and rutile inclusions. Along fractures, garnet is altered to chlorite. Plagioclase is subhedral and commonly sericitized; it shows no evident zoning under the microscope. K-feldspar is less altered, has diffuse microcline twinning, and incipient undulose extinction (see Table 1 for sample mineralogy).

2) Hornblende-bearing quartzofeldspathic gneiss intercalated with amphibolites (Figure 2). This gneiss shows a banded texture, decimeter-sized isoclinal folds, and boudin structures formed by mafic minerals. The main difference between this particular gneiss and garnet-free amphibolite is the higher amount of felsic minerals in the gneiss compared to the amphibolite.

3) Towards the southeast, approximately 1.5 km from Finca Custepec, on a tributary stream of Las Nubes river, another type of quartz-feldspar gneiss crops out. It contains microcline and has a more homogeneous appearance compared to the layered gneisses within the amphibolites. Therefore, we suggest this gneiss had probably an igneous protolith.

Marbles and calcsilicate rocks

Marbles and calcsilicate rocks crop out in various wedge-shaped lenses or boudins interlayered with amphibolite. Banded and strongly folded marbles are composed of coarse-grained calcite, mm-sized orange micas with minor pyroxene, quartz and some garnet.

Granitoids

Almost undeformed isotropic granitoids of mostly tonalitic composition intrude the Custepec Unit to the North and to the South (Figure 2). Tens of centimeters to meter-sized xenoliths of amphibolite and gneiss from the Custepec Unit are common in the granitoids, especially close to their intrusive contacts.

Structural features

Figure 4a shows an equal area projection plot of foliation planes from the Custepec area. Although many foliation planes are randomly oriented, we calculated a great circle

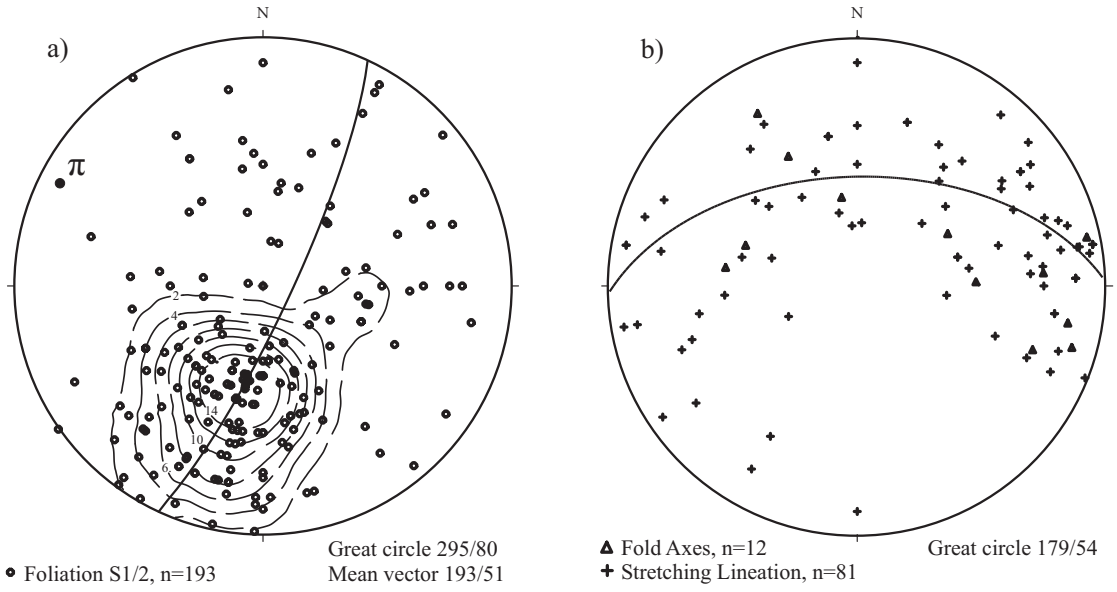

Figure 4. Equal area projection plot of structures from the Custepec area. a: Foliation planes, b: fold axes (F_2) and stretching lineations (L_2). Great circles and mean vectors calculated with Stereonet for Windows, version 1.2.

that dips towards the WNW (295/80). Besides that, most of the foliation planes dip towards the north, indicating that regional folds are reclined towards the south. Locally, the main foliation (S_1) is folded by isoclinal centimeter-to decimeter-wide folds (F_2, Figure 5). Fold axes and scarcely observed stretching lineations have varying directions, indicating refolding during a third deformation D_3. Either well delimited or diffuse ductile shear zones, affecting both amphibolite and gneiss, are characterized by grain size reduction and recrystallization of quartz together with plagioclase porphyroclasts that range in size from 1 to 10 mm. These shear zones indicate a later stage (post D_2 or D_3) ductile deformation under low-grade metamorphic conditions. Most of the observed shear zones display a mylonitic foliation that dips moderately towards the NW with sub-horizontal lineations. Kinematic indicators of shear sense are incongruent, but in most cases a dextral shear sense was determined, indicating movements of the hanging wall towards the E-NE. Mylonites with similar kinematics have been reported by Schaaf *et al.* (2002) from the northern central Chiapas Massif.

MINERAL CHEMISTRY AND THERMOBAROMETRY

We have chosen two samples for pressure and temperature estimates: a sillimanite+garnet-bearing biotite gneiss (JMC-68b), and a garnet-amphibolite (JMC-01). Representative electron microprobe analysis used for calculations are shown in Tables 2, 3 and 4.

Pelitic gneiss (sample JMC-68b)

The compositional profile of garnet in the pelitic gneiss allows recognizing three zones, as shown in Figure 6. From core to rim, we named these zones 1, 2, and 3. Zone 1 is a nearly homogeneous core with an average composition of $Alm_{78.9}$–$Prp_{15.4}$–$Grs_{2.2}$–$Sps_{2.7}$. A transition is revealed at the border of zone 1 by an increase in Ca content from 2.1 mol% in zone 1 to 5.0 mol% in zone 2. Although zone 2 contains higher Ca concentration, the ratios among Fe, Mg, and Mn are similar to those of zone 1. Zone 2 is also characterized by numerous and relatively large quartz inclusions. In zone 1 and 2, the garnet shows rather homogeneous Mg# = 0.16. Zone 3 is the portion of the garnet rim in which Fe and Mn increase and Mg decreases.

We interpret this garnet profile in terms of two distinct stages of garnet growth (zones 1 and 2) and a third stage of retrogression (zone 3). The first stage (zone 1) involved garnet growth during prograde metamorphism. The second stage (zone 2) of garnet growth was produced by a reaction with excess silica that left quartz inclusions in the garnet (Figure 6) and an increase of the grossular component by ~2.9 Mol%. Calcium increase may have been the result of garnet growth during a phase of isobaric cooling (following contours of grossular isopleths after Spear *et al.*, 1990). Finally, Fe increase and Mg decrease in zone 3 are characteristic of retrogression conditions. The small Mn spike near the garnet rim in zone 3 indicates that garnet was consumed during a retrograde net-transfer reaction (Kohn and Spear, 2000). The excess Fe released from the consumed garnet must have been reabsorbed by matrix minerals, and most likely modified the original composition of matrix biotite.

Biotite occurs both as a modally abundant matrix phase and as inclusions in garnet porphyropblasts (Figure 7a and b). Measured matrix biotite has an average Mg# (Mg/Mg+Fe) of 0.41. The biotite inclusions in garnet show more variation in Mg#, ranging from 0.39 to 0.67, whereas grains touching garnet have a Mg# of 0.42, similar to that of the matrix biotite (Figure 8). Titanium concentrations in biotite also vary significantly, being lower in grains touching garnet and higher in matrix biotites. An exception is a biotite inclusion in garnet that contains more than 0.6 cations per 22 oxygen formula unit (Figure 8). This biotite has also the highest Mg# of 0.67.

In order to obtain reliable thermobarometric estimates,

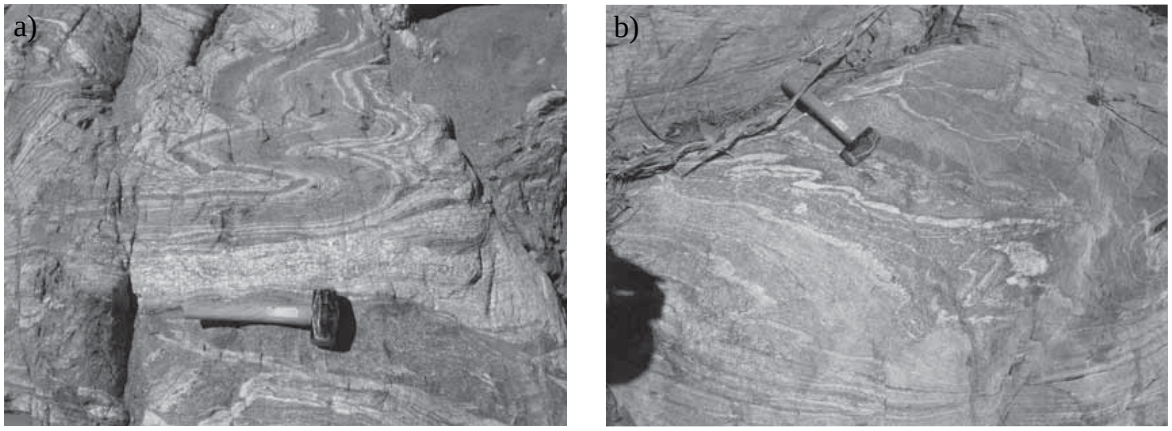

Figure 5. a: Isoclinal decimiter-to centimeter-wide folds in ampbibolite; b: hornblende-bearing quartzofeldspathic gneiss.

Table 2. Representative analysis of minerals from metapelite (Sample JMC-68b), Custepec Unit, Chiapas Massif Compex.

	Garnet				Ilmenite	
	Core	**Rim**	**446**	**437-440**	**441-445**	**453-455**
wt.%						
SiO_2	37.75	37.08	38.26	36.63	0.11	0.27
TiO_2	0.02	0.01	0.00	1.19	0.05	0.11
Al_2O_3	21.94	21.48	21.85	21.18	51.81	49.63
FeO	32.86	35.43	31.35	33.24	45.01	45.35
MnO	1.06	1.27	0.10	0.93	1.81	1.82
MgO	6.42	3.77	6.61	5.45	0.07	0.10
CaO	1.02	1.93	1.55	0.97	0.00	0.01
					Na_2O 0.09	0.11
Oxide totals	101.07	101.00	100.38	99.60	K_2O 0.00	0.00
Formula basis 12 oxygens					Oxide totals 98.96	97.49
Si	2.95	2.96	3.00	2.93		
Ti	0.00	0.00	0.00	0.00	*Formula basis 3 oxygens*	
Al	2.02	2.02	2.02	1.99	Si 0.003	0.007
Fe	2.15	2.36	2.06	2.22	Ti 0.002	0.003
Mn	0.07	0.09	0.01	0.06	Al 0.994	0.973
Mg	0.75	0.45	0.77	0.65	Fe 0.960	0.988
Ca	0.09	0.16	0.13	0.08	Mn 0.039	0.040
					Mg 0.003	0.004
X_{Py}	0.245	0.146	0.261	0.215	Ca 0.000	0.000
X_{Alm}	0.704	0.772	0.693	0.736	Na 0.002	0.003
X_{Grs}	0.028	0.054	0.044	0.028	K 0.000	0.000
X_{Sps}	0.023	0.028	0.002	0.021		

Numbers refer to the microprobe analysis number. Analysis of ilmenite are from two different grains included in garnet. Analysis 446 and 437-440 of garnet were made near to ilmenite.

the effect of garnet resorption needs to be taken into account. This is accomplished by calculating the amount of Mn that was forced back into the garnet rim during resorption, which is a proxy to determine the volume of dissolved garnet (Kohn and Spear, 2000). Following the procedure by Kohn and Spear (2000), we calculated ~16 vol% of garnet was consumed during retrogression. This method yields an estimate of the composition of the biotite that was in equilibrium with garnet core. In contrast, to estimate retrogression conditions, the outermost composition of garnet and matrix biotite (in contact with garnet) need to be used.

Plagioclase grains are subhedral and show high integrity. No zoning was observed under the microscope, but chemical profiles show progressive zoning with a decrease in An content from core to rim of crystals (not shown). K-feldspar is present as a minor constituent.

Secondary titanite formed from rutile indicates a decompression process. A later stage of retrograde metamorphism is also marked by chlorite formation from garnet, sericitization of plagioclase, and breakdown of sillimanite into fine-grained white mica.

For the metapelite (sample JMC-68b), metamorphic temperature conditions were estimated on the basis of the Fe^{+2}-Mg exchange vector. Compositions of minerals to estimate metamorphic conditions were calculated as described above. Pressure conditions were calculated using both the GASP and GRAIL barometers. The intersection of the GARB thermometer (calibration of Ganguly and Saxena, 1984) with the GRAIL barometer (calibration of Bohlen *et al.*, 1983) yields equilibrium conditions of 800 ºC and 8.6–9.3 kbar (Figure 9), which correspond to homogenization after the second phase of garnet growth.

To calculate metamorphic conditions during retrogression, the compositions of garnet rims and biotite in contact with garnet were used. As expected, this yielded lower temperatures (Figure 9) compared to the garnet core and corrected biotite pair. Intersection of GARB thermometer with GASP barometer (calibration of Ganguly and Saxena, 1984) yields 675 ºC and 5.5 kbar. Assuming that biotite in contact with the garnet rim preferentially re-equilibrated during retrogression, the lower temperatures can be interpreted as representing metamorphic conditions during retrogression (Figure 9).

Amphibolite (sample JMC-01)

Garnet amphibolite JMC-01 contains brown, poikiloblastic amphibole. Cores are Ti-rich ferropargasite (Figure 7c) rimmed by green to olive-green ferrotschermakite (amphibole classification after Leake *et al.*, 1997; Figure 10) ; amphibole composition calculated using software by Esawi, 2004). Both brown and green hornblende are partly retrogressed to chlorite and epidote. Inclusions in hornblende are mainly apatite and titanite. Titanite formed from hornblende as a result of retrogression. Inclusions in

Table 3. Representative analysis of minerals from metapelite (Sample JMC-68b), Custepec Unit, Chiapas Massif Complex.

	Biotite			Plagioclase	
	Matrix	**Touching Grt**	**Included in Grt**	**Core**	**Rim**
wt.%				wt.%	
SiO_2	34.38	34.69	35.49	SiO_2 60.09	60.79
TiO_2	3.45	1.43	2.64	Al_2O_3 23.77	23.72
Al_2O_3	17.89	19.06	17.30	FeO 0.03	0.03
FeO	20.53	21.75	18.99	CaO 6.54	6.22
MnO	0.09	0.11	0.03	Na_2O 7.53	8.33
Cr_2O_3	0.01	0.00	0.00	K_2O 0.38	0.21
MgO	7.94	8.93	10.40		
CaO	0.01	0.02	0.00		
Na_2O	0.10	0.04	0.06		
K_2O	8.98	9.12	9.85		
Total	93.38	95.16	94.74	Total 98.34	99.30
Formula basis 22 oxygens				*Formula basis 8 oxygens*	
Si	5.38	5.35	5.45	Si 2.72	2.73
Al^{IV}	2.62	2.65	2.55	Al 1.27	1.25
				Fe^{II} 0.00	0.00
Al^{VI}	0.69	0.81	0.58	Ca 0.32	0.30
Ti	0.41	0.17	0.30	Na 0.66	0.72
Fe^{II}	2.69	2.80	2.44	K 0.02	0.01
Mn	0.01	0.01	0.00		
Mg	1.85	2.05	2.38	Total 4.99	5.02
Ca	0.00	0.00	0.00		
Na	0.03	0.01	0.02	X_{An} 0.317	0.289
K	1.79	1.79	1.93	X_{Ab} 0.661	0.700
				X_{Or} 0.022	0.012
Mg/Mg+Fe	0.41	0.42	0.49		

Table 4. Representative analysis of minerals from garnet amphibolite (Sample JMC-01), Custepec Unit, Chiapas Massif Complex.

	Hornblende			Plagioclase			Garnet	
	212 core	**224 rim**		**196 core**	**208 rim**		**225 core**	**240 rim**
wt.%			wt.%			wt.%		
SiO_2	45.03	44.65	SiO_2	58.41	57.76	SiO_2	37.64	38.06
TiO_2	0.97	0.92	TiO_2	0.01	0.00	TiO_2	0.04	0.05
Al_2O_3	9.93	9.96	Al_2O_3	25.78	26.35	Al_2O_3	20.63	21.12
FeO	18.43	18.68	FeO	0.03	0.12	FeO	27.13	26.29
MnO	0.28	0.44	MnO	0.00	0.00	MnO	2.32	2.69
Cr_2O_3	0.01	0.00	Cr_2O_3	0.00	0.00	Cr_2O_3	0.03	0.02
MgO	9.86	9.23	MgO	0.00	0.00	MgO	3.90	5.11
CaO	11.15	11.38	CaO	6.55	6.81	CaO	7.29	6.40
Na_2O	1.25	0.90	Na_2O	7.38	7.11			
K_2O	1.20	1.04	K_2O	0.11	0.09			
Total	98.12	97.20	Total	98.27	98.26	Total	98.97	99.80
Formula basis 23 oxygens			*Formula basis 8 oxygens*			*Formula basis 12 oxygens*		
Si	6.66	6.68	Si	2.65	2.62	Si	3.009	2.999
Al^{IV}	1.34	1.32	Al	1.38	1.41	Ti	0.003	0.003
			Fe^{II}	0.00	0.00	Al	1.944	1.962
Al^{VI}	0.39	0.44	Ca	0.32	0.33	Fe	1.814	1.732
Fe^{III}	0.60	0.56	Na	0.65	0.63	Mn	0.157	0.180
Ti	0.11	0.10	K	0.01	0.01	Mg	0.466	0.601
Cr	0.00	0.00		4.99	4.99	Ca	0.624	0.540
Fe^{II}	1.68	1.78						
Mn	0.04	0.06	X_{An}	0.327	0.344	X_{Py}	0.152	0.197
Mg	2.17	2.06	X_{Ab}	0.667	0.651	X_{Alm}	0.593	0.567
Ca	1.77	1.82	X_{Or}	0.006	0.006	X_{Grs}	0.204	0.177
Na	0.36	0.26				X_{Sps}	0.051	0.059
K	0.23	0.20						

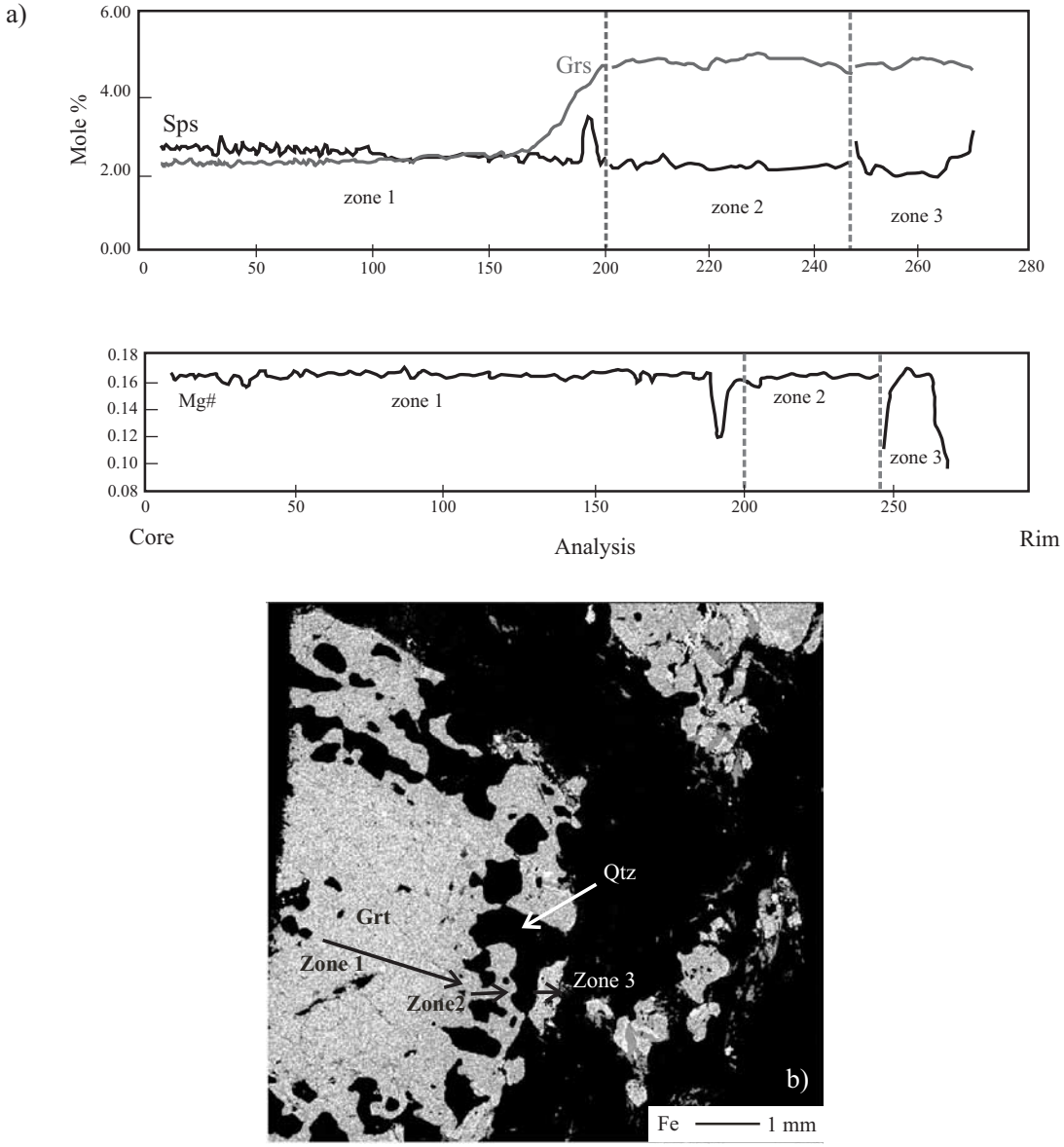

Figure 6. a: Chemical composition of a profile on garnet (core to rim) from the metapelite (sample JMC-68b). b: X-ray map of Fe on garnet from sample JMC-68b; light grey and white is rich in Fe (*e.g.*, garnet), black is low in Fe (*e.g.*, quartz). Note that poikiloblastic outer part of garnet coincides with increase of X_{Grs} in the profile and decrease in Mg# (a).

hornblende are mainly apatite and titanite. Biotite is also present in this rock but it is almost completely retrogressed to chlorite.

Plagioclase is subhedral, partially sericitized and displays undulose extinction. Although zoning is not petrographically visible, compositional profiles show oscillatory zoning with a slight increase of An content towards the rim. Fine-grained quartz crystals are smaller than other major constituents of this sample, and display incipient undulose extinction.

A different generation of amphibole is greenish-blue to bluish-green hastingsite (Figure 7). These amphiboles rarely occur in the felsic matrix where they are surrounded by plagioclase, in contact with retrogressed biotite, and as inclusions within garnet porphyroblasts. Probably, these are prograde amphiboles that grew at the same time as the porphyroblasts that engulf them and rarely survived in the matrix.

The chemical composition of garnet is nearly homogeneous averaging $Alm_{57.0}$–$Prp_{17.5}$–$Grs_{17.5}$–$Sps_{5.0.}$ This feature indicates that garnet was probably rehomogenized during high-grade metamorphism and remained almost unaffected by later retrogression reactions. The peak mineral assemblage of this rock is hornblende + plagioclase + biotite + quartz.

For the garnet-amphibolite, pressure conditions were estimated on the basis of the garnet + plagioclase + hornblende + quartz assemblage (Kohn and Spear, 1990).

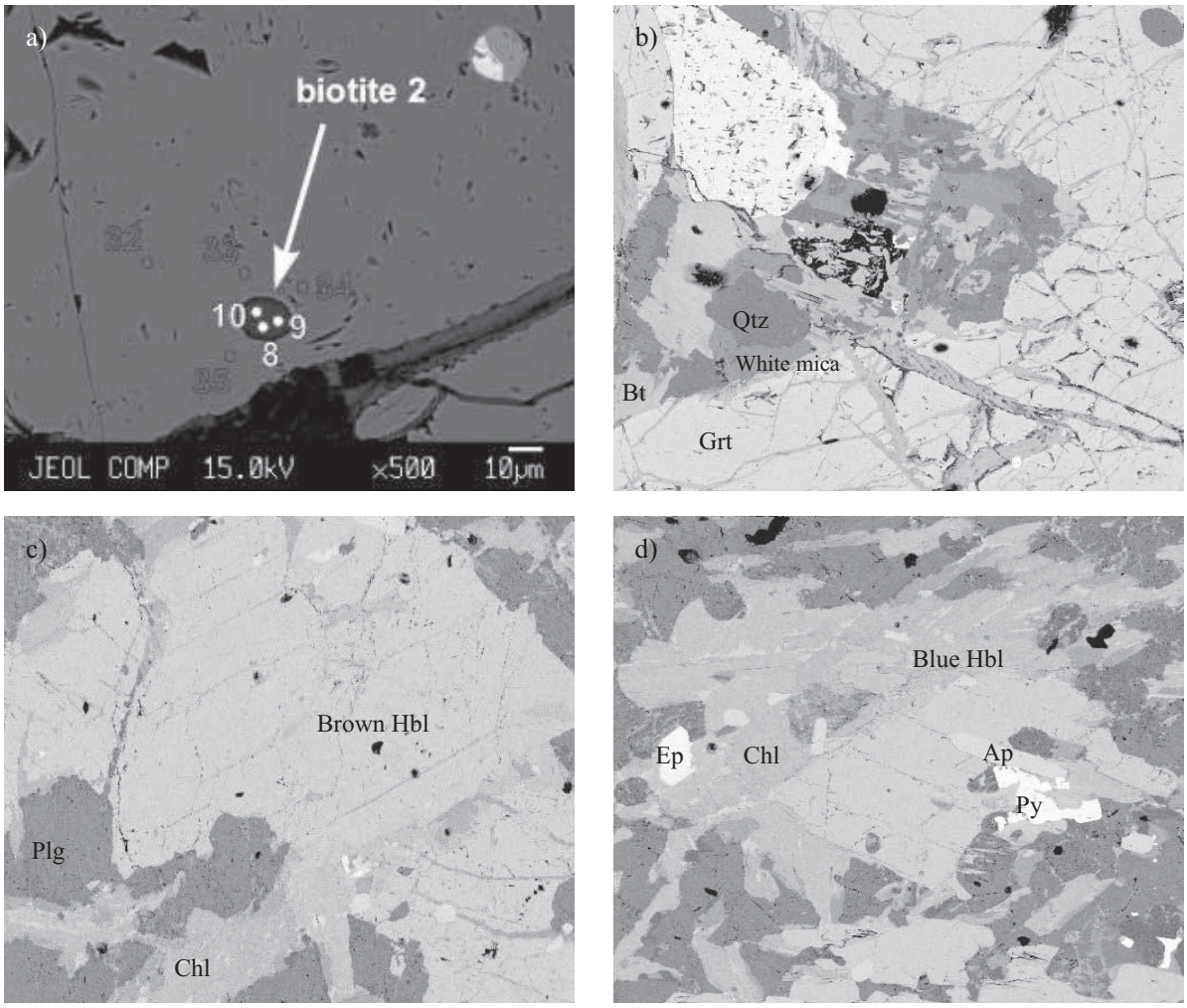

Figure 7. Backscattered electron images. a and b: Biotite inclusions in garnet from metapelite (sample JMC-68b), biotite 2 in (a) has the highest measured Ti content. c: Pargasite from garnet-bearing amphibolite (sample JMC-01). d: Greenish-blue hastingsite from garnet-bearing amphibolite. Ap: apatite; Bt: biotite; Chl: chlorite; Ep: epidote; Grt: garnet; Hbl: hornblende; Plg: plagioclase; Py: pyrite; Qtz: quartz.

Temperature conditions were calculated using the hornblende + plagioclase thermometer of Holland and Blundy (1994).

Thermobarometric calculations employing brown Ti-rich ferropargasite, garnet and plagioclase cores yielded temperature conditions of 718 ºC and a pressure of 8.2 kbar (Figure 11). Rims of the same minerals (Figure 11) yielded a temperature of 680 ºC and a pressure of 7.8 kbar.

Sm-Nd GEOCHRONOLOGY

In an effort to constrain the timing of metamorphism in the Custepec Unit, we measured Sm and Nd isotope ratios for garnet and whole rock from a garnet amphibolite (CB45, Figure 2). The results are shown in Table 5. Garnet of this sample yielded a $^{147}Sm/^{144}Nd$ ratio (0.7811) about ten times higher compared with the whole rock analysis (0.0773), which renders this pair useful for calculating a garnet–whole rock age. The slope of a line connecting garnet and whole rock data in a $^{147}Sm/^{144}Nd$ *vs.* $^{143}Nd/^{144}Nd$ plane yields an age of 267.9 ± 9.4 Ma (2σ) and an initial ε_{Nd} of -8.8. The latter, together with a T_{DM} model age of ~1200 Ma (Table 5), indicate that the garnet-amphibolite is mostly made of recycled continental crust.

DISCUSSION

The pressure-temperature-time path of the Custepec Unit

On the basis of our thermobarometric data,the garnet-whole rock age, and a previously published U-Pb age on metamorphic and anatectic zircons (Weber *et al.*, 2007) we propose a pressure-temperature-time path for the Custepec Unit as shown in Figure 12.

As discussed above, there were two stages of garnet

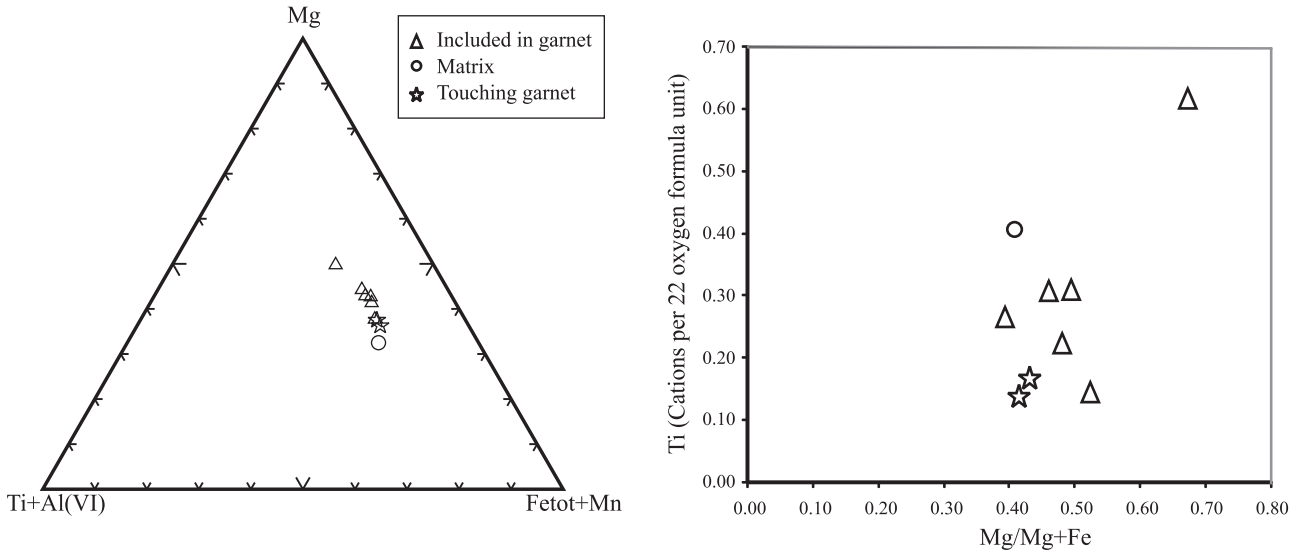

Figure 8. Chemical variation diagrams of biotite from metapelite (sample JMC-68b). Note: Mg# (Mg/Mg+Fe) varies significantly in inclusions. Ti concentration in biotite also varies, being lower in grains touching garnet and higher in matrix biotites with the exception of an inclusion (see Figure 7a) that contains more than 0.6 Ti cations per 22 oxygen formula unit.

growth (zone 1 and zoned 2; Figure 6) and a third stage of retrogression accompanied by garnet consumption (zone 3). The second stage of garnet growth and retrogression, impeded the recovery of mineral compositions established at peak metamorphic conditions. The similarity in composition and Mg# from zone 1 and zone 2 of garnet leads us to think that temperature conditions during the second stage of garnet growth caused Fe, Mg and Mn to re-homogenize throughout garnet except at the outermost rim. The comparatively slow rates of Ca diffusion enabled the preservation of the Ca zoning. Therefore we interpret temperature obtained from garnet core and corrected biotite pairs together with the corresponding pressure from the GRAIL barometer (Figure 12) as an estimate of the conditions during the second stage of garnet growth. If this assumption is true then the temperature from the first stage of garnet growth and from the peak are unkown. Calcium increase may be explained by a stage of garnet growth at lower temperature than the metamorphic peak, but similar pressure (Spear *et al.,* 1990), being indicative of a phase of isobaric cooling following the metamorphic peak. Similar pressures and lower temperatures obtained from the amphibolite appear to confirm this P-T path tendency (Figure 12).

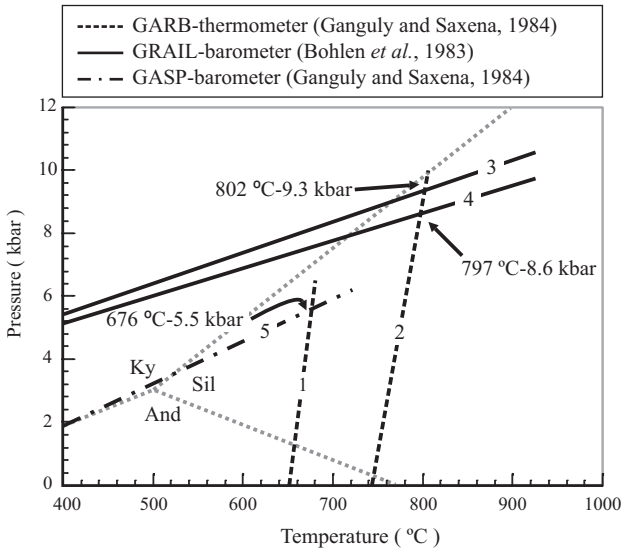

Figure 9. Temperature and pressure estimates for sample JMC-68b (garnet-sillimanite-biotite gneiss). Numered lines correspond to calculations using different mineral sub-assemblages. 1: Garnet core (average Mg #) with matrix biotite corrected for garnet dissolution (after Khon and Spear, 2000); 2: garnet rim with biotite touching garnet; 3: garnet (analysis #446) with ilmenite (#441-445) included in garnet; 4: garnet (#437-440) with ilmenite (#441-445) included in garnet; 5: garnet rim with plagioclase rim. Intersection of lines 2-3 and 2-4 are interpreted as the minimum peak temperature. Intersections of lines 1-5 correspond to retrograde conditions. For analysis number and mineral compositions see Tables 2 and 3. Andalusite (And)-Kyanite (Ky)-Sillimanite (Sil) invariant point according to Holdaway (1971).

The temperature calculated from ferrotschermakite and plagioclase rims (680 ºC) is in good agreement with the temperature of retrogression calculated for the metapelite, but the corresponding pressure conditions are fairly above expected (Figure 12, ferrotschermakite, plagioclase and garnet rims). However, this pressure calculation may be affected by the presence of Ca-bearing phases other than plagioclase, especially secondary phases like epidote and titanite, whose Ca content is not considered in the barometer.

The U-Pb age can be interpreted as the time of zircon crystallization from the neosome and metamorphic overgrowth in the paleosome. Solidus temperature of a tonalitic to granodioritic magma can be assumed to lie significantly below 800–750 ºC at H_2O pressures above 8 kbar. This implies that the U-Pb age can be regarded as the time of

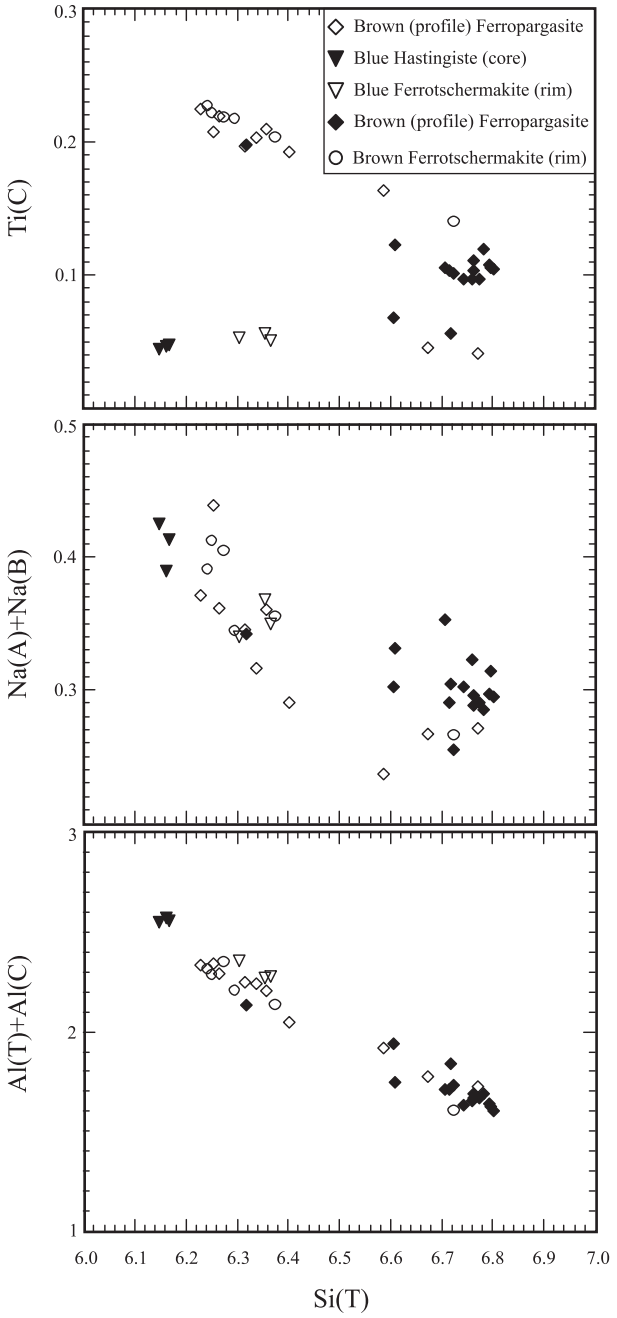

Figure 10. Chemical composition of amphiboles analyzed from the amphibolite (sample JMC-01). Open and filled diamonds correspond to different profiles on brown amphibole, open circles are analyses from the rim of brown amphibole. Amphibole classification after Leake *et al.* (1997).

crystallization of the partially melted portion of the rock, which in turn marks a later stage of metamorphic evolution after the metamorphic peak. Since our Sm-Nd garnet-whole rock age is significantly older than the U-Pb zircon age, we interpret the Sm-Nd garnet-whole rock age as an average age of garnet formation. The latter interpretation implies that the closure temperature for Sm and Nd diffusion in garnet was >750–800 ºC (*e.g.*, Cohen *et al.*, 1988; Hensen and Zhou, 1995; Becker, 1997).

Regional tectonic implications

Our detailed geologic and petrographic study of the Custepec Unit revealed that metamorphic conditions documented in the rocks from the Custepec Unit are considerably higher than those in the Sepultura Unit, which constitutes the host rocks for the Permian-Triassic plutons in the northwestern part of the Chiapas Massif (Weber *et al.*, 2002). Besides, the ubiquity of amphibolites in the Custepec Unit strongly suggests this pre-batholithic sequence is different from the Sepultura Unit, in which amphibolites are mostly absent. The presence of metapelitic rocks, calcsilicates, and marbles either as intercalations, inclusions, and blocks or as mapable units tens to hundreds of meters in size, allows concluding that the Custepec Unit is of sedimentary origin, with the amphibolites representing volcanosedimentary protoliths. It cannot be totally ruled out that the protoliths of the amphibolites were igneous rocks like gabbros, and the metapelites, calcsilicates, and marbles might be xenoliths from supracrustal rocks assimilated by the mafic plutonic rocks. However, the abundance of Mesoproterozoic zircons in the amphibolites (Weber at al., 2007) and its Nd isotopic composition (this work) argue against gabbroic protoliths for the amphibolites of the Custepec Unit.

Regardless the protolith origin, our data indicate that the Custepec Unit represents a lower crustal level with respect to the Sepultura Unit. A comprehensive record of structural data from the entire Chiapas Massif is not available but the observed difference in the exposed crustal level can be explained by the following processes: 1) the entire sequence was tilted towards the NW; 2) the Custepec Unit represents a nappe thrusted over the low-pressure units (Sepultura), perhaps during the retrograde event; or 3) inverse faulting due to batholith intrusion caused uplift of lower crustal protoliths in the Custepec Unit. Pervasive

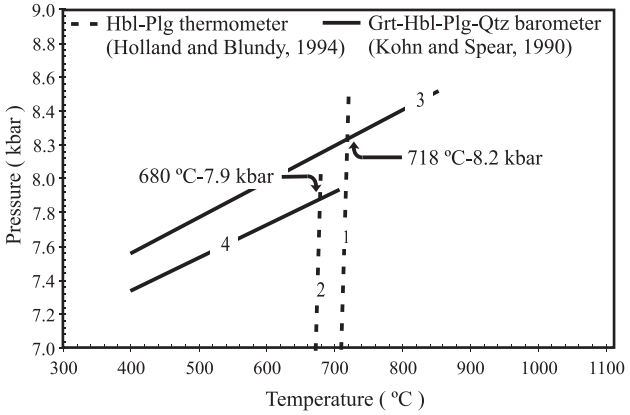

Figure 11. Temperature and pressure estimates for garnet-bearing amphibolite (Sample JMC-01). - Numbered lines correspond to different calculations using either core or rim of mineral grains. 1: hornblende (#212) and plagioclase (#196) core minerals; 2: hornblende (#224) and plagioclase (#208) rims; 3: hornblende (#212), plagioclase (#196), and garnet (#240) cores; 4: hornblende (#224), plagioclase (#208), and garnet (#225) mineral rims. For analyses number and mineral compositions see Table 4.

Table 5. Sm and Nd element concentrations and isotopic compositions of garnet and whole rock for sample CB45 from the Custepec Unit, Chiapas, N 15.71474º, W 92.95560º.

Sample	Sm (ppm)	Nd (ppm)	$^{147}Sm/^{144}Nd$[a]	$^{143}Nd/^{144}Nd$	$\pm1\sigma$[b]	$\varepsilon Nd_{(i)}$	T_{DM} (Ma)	Garnet-whole rock age (±2σ)
Whole rock	11.01	86.06	0.0773	0.511975	0.000013	-8.8	1188	
Garnet ID	4.94	3.82	0.7811					
Garnet CR				0.513208	0.000018			267.9 ± 9.4 Ma

ID = isotope dilution run; CR = composition run. [a] = Uncertainties at $1\sigma_{rel}$: $^{147}Sm/^{144}Nd$ ± 0.1%; [b] = number of measured isotope ratios $n = 60$ ($\sigma_m = \pm (\sigma/\sqrt{n})$); [c] = Nd model age after DePaolo (1981); element concentrations are ± 1%.

E-W trending foliation and dip-directions indicating southern vergence of folds suggest a fold-thrust system rather than exhumation by vertical tectonics. On the other hand, Late Cretaceous subduction and collision of the Chortís against the Maya block (Harlow *et al.*, 2004) and Neogene southeastward movement of the Chortís block along the continental margin of southern Mexico (*e.g.* Burkart and Self, 1985; Muehlberger and Ritchie, 1975), could have caused higher uplift in the southeastern compared to the northwestern part of the Chiapas Massif, resulting in the exhumation of lower crustal levels towards the southeast and, hence, this scenario favors the assumption that the Chiapas Massif is tilted towards the northwest. However, in the Motozintla area (Figure 1), metasedimentary rocks with provenances similar to those from the Custepec Unit only display low- to medium-grade metamorphic conditions (Weber *et al.*, 2008).

As discussed above, the garnet-whole rock age of 268 ± 9 Ma probably reflects an average of garnet formation. Hence, orogenesis in the Chiapas Massif started in the late Early Permian and can be linked either with the latest stage of Alleghanian Orogeny (Viele and Thomas, 1989) or with the onset of subduction of the proto-Pacific. Weber *et al.* (2008) consider the development of a short-lived westward-dipping subduction beneath Oaxaquia as a plausible explanation for arc magmatism in the Chiapas Massif during the Early Permian. In this scenario, the metamorphic peak in the Custepec Unit might be linked with the late Early Permian westward dipping subduction, deformation (D_1) and magmatism. Following this model, convergence culminated in the collision of the western Maya block with eastern Oaxaquia in the Late Permian. In the Custepec Unit, after a period of isobaric cooling, this collision event is probably documented by intense folding with southern vergence (D_2) and possible southward thrusting of the Custepec Unit over less metamorphosed units (like the Sepultura Unit), which caused a phase of rapid uplift and the first retrogression under amphibolite facies conditions. The latter event was followed by the intrusion of voluminous calc-alkaline plutons that constitute most of the Chiapas Massif, in the

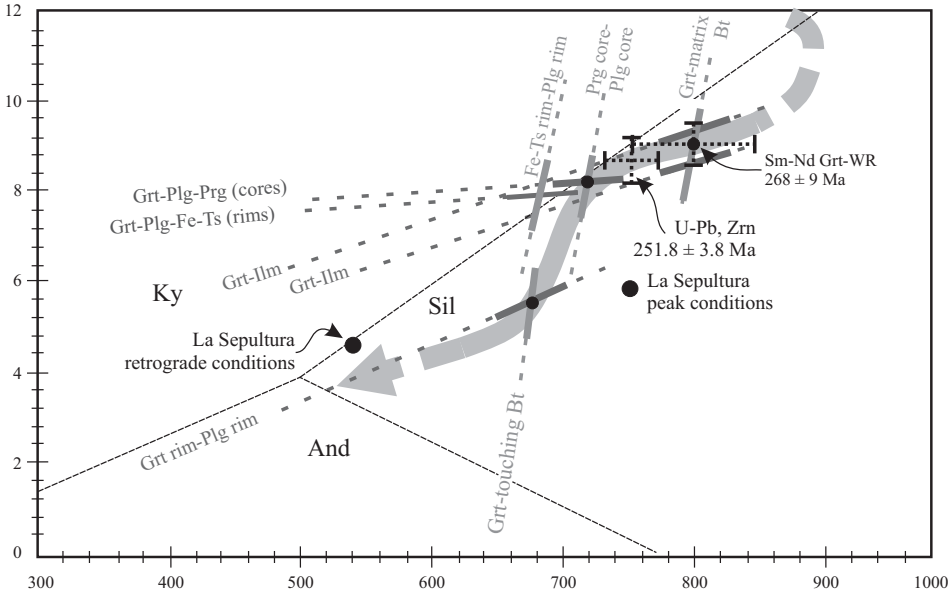

Figure 12. P-T-t trajectory model for the Custepec Unit interpreted from pressure and temperature estimates from samples JMC-68b and JMC-01 (Figure 9 and 11) and the Sm-Nd garnet – whole rock age (Table 5), as well as the zircon U-Pb age (Weber et al., 2007). For further explanation see text. Prg: pargasite; Fe-Ts: ferrotschermakite.

Late Permian to Early Triassic (Damon *et al.* 1981; Schaaf *et al.* 2002), as a result of the eastward subduction. These intrusions probably affected the basement rocks not only by further retrogression under greenschist facies but also by deformation (D_3) and reorientation of structural features. The beginning of crustal extension and seafloor spreading led to the rotation of the Maya block, starting in the Early Triassic (Dickinson and Lawton, 2001). This event is probably responsible for the development of dextral ductile shear zones in the Custepec Unit.

ACKNOWLEDGEMENTS

This work was supported by CONACYT project D41083-F, DFG/BMZ collaboration project HE2893/3,4-1, and CICESE internal project 644111. We express gratitude to Susana Rosas-Montoya and Víctor Pérez-Arroyoz (CICESE) for their help in sample and thin sections preparation, and mineral separation. We wish to thank J. Morales-Contreras, G. Solís-Pichardo, and P. Schaaf from the Laboratorio Universitario de Geoquímica Isotópica, Universidad Nacional Autónoma de México, Mexico City, for assistance in Sm- Nd isotope data acquisition. We thank Oscar Talavera-Mendoza and anonymous reviewer for their helpful comments and detailed criticism that helped improve the manuscript. We are grateful to Armando Pohlenz and Don Martin Pohlenz for their hospitality and their logistical support at the Finca Custepec.

REFERENCES

Bateson, J.H., Hall, I.H.S., 1977, The geology of the Maya Mountains, Belize: Institute of Geological Science, Her Majesty´s Stationery Office, Overseas Memoir 3, 43.

Becker, H., 1997, Sm-Nd garnet ages and cooling history of high-temperature garnet peridotite massifs and high-pressure granulites from lower Austria: Contributions to Mineralogy and Petrology, 127, 224-236.

Bohlen, S.R., Wall, V.J., Boetcher, A.l., 1983, Experimental investigations and geological applications of equilibria in the system FeO-TiO_2-Al_2O_3-SiO_2-H_2O: American Mineralogist, 68, 1049-1058.

Burkart, B., 1983, Neogene North American-Caribbean plate boundary across northern central america: Offset along the Polochic fault: Tectonophysics, 99, 251-270.

Burkart, B., Self, S., 1985, Extension and rotation of crustal blocks in northern Central America and effect on the volcanic arc: Geology, 13 (1), 22-26.

Campa, M.F., Coney, P.J., 1983, Tectono-stratigraphic terranes and mineral resource distributions in Mexico: Canadian Journal of Earth Sciences, 20, 1040-1051.

Cohen, A.S., O'Nions, R.K., Siegenthaler, R., Griffin, W.L., 1988, Chronology of the pressure history recorded by granulite terrane: Contributions to Mineralogy and Petrology, 98, 303-311.

Damon, P.E., Shafiqullah, M., Clark, K., 1981, Age trends of igneous activity in relation to metallogenesis in the southern Cordillera, *in* Dickinson, W., Payne, W.D. (eds.), Relations of Tectonics to Ore Deposits in the Southern Cordillera: Tucson, Arizona, Arizona Geological Society Digest, 14, 137-153.

Dengo, G., 1985, Mid America; tectonic setting for the Pacific margin from southern Mexico to northwestern Colombia, *in* Nairn. A.E.M., Stehli, F.G. (eds.), The Ocean Basins and Margins, 7a. The Pacific Ocean: New York, Plenum Press, 123-180.

Dickinson, W.R., Lawton, T.F., 2001, Carboniferous to Cretaceous assembly and fragmentation of Mexico: Geological Society of America Bulletin, 113(9), 1142–1160.

Ducea, M.N., Gehrels, G.E., Shoemaker, S., Ruiz, J., Valencia, V.A., 2004, Geologic evolution of the Xolapa Complex, southern Mexico: Evidence from U-Pb zircon geochronology: Geological Society of America Bulletin, 116 (7-8), 1016-1025.

Elías-Herrera, M., Ortega-Gutiérrez, F., 2002, Caltepec fault zone: An early Permian dextral transpressional boundary between the Proterozoic Oaxacan and Paleozoic Acatlán complexes, southern México, and regional tectonic implications: Tectonics, 21, 1-19.

Esawi, E.K., 2004, AMPH-CLASS: An Excel spreadsheet for the classification and nomenclature of amphiboles based on the 1997 recommendations of the International Mineralogical Association: Computers and Geosciences, 30, 753-760.

Ganguly, J., Saxena, S.K., 1984, Mixing properties of aluminosilicate garnets: constraints from natural and experimental data, and applications to geothermo-barometry: American Mineralogist, 69, 88-97.

Harlow, G.E., Hemming, S.R., Avé Lallemant, H.G., Sisson, V.B., Sorensen, S.S., 2004, Two high-pressure-low-temperature serpentinite-matrix mélange belts, Motagua fault zone, Guatemala: A record of Aptian and Maastrichtian collisions: Geology, 32(1), 17-20.

Hensen, B.J., Zhou, B., 1995, Retention of isotopic memory in garnets partially broken down during an overprinting granulite-facies metamorphism; implications for the Sm-Nd closure temperature: Geology, 23(3), 225-228.

Hiller, R., Weber, B., Hecht, L., Ortega-Gutiérrez, F., Schaaf, P., López-Martínez, M., 2004, The 'Sepultura' unit – A medium to high grade metasedimentary sequence in the Chiapas Massif, SE México (abstract), *in* Reunión Nacional de Ciencias de la Tierra, Libro de Resúmenes, Querétaro, México: GEOS, 24(2), 297-298.

Hodges, K.V., Spear, F.S., 1982, Geothermometry, geobarometry and the Al_2SiO_5 triple point at Mt. Moosilauke, New Hampshire: American Mineralogist, 67, 1118-1134.

Holdaway, M.J., 1971, Stability of andalusite and the aluminum silicate phase diagram: American Mineralogist, 271, 97-131.

Holland, T.J.B., Blundy, J., 1994, Non-ideal interactions in calcic amphiboles and their bearing on amphibole-plagioclase thermometry: Contributions to Mineralogy and Petrology, 116(4), 433-447.

Keppie, J.D., Dostal, J., Murpy, J.B., Nance, R. D., 2008, Synthesis and tectonic interpretation of the westernmost Paleozoic Variscan orogen in southern Mexico: From rifted Rheic margin to active Pacific margin: Tectonophysics, 461(1-4), 277-290, doi:10.1016/j.tecto.2008.01.012.

Kohn, M.J., Spear, F.S., 1990, Two new geobarometers for garnet amphibolites, with applications to southeastern Vermont: American Mineralogist, 75, 89-96.

Kohn, M.J., Spear, F.S., 2000, Retrograde net transfer reaction insurance for pressure-temperature estimates: Geology, 28(12), 1127-1130.

Leake, B.E., Woolley, A.R., Arps, C.E.S., Birch, W.D., Gilbert, M.C., Grice, J.D., Hawthorne, F.C., Kato, A., Kisch, H.J., Krivovichev, V.G., Kees Linthout, J.L., Mandarino, J.A., Maresch, W.V., Nickel, E.H., Rock, N.M.S., Schumacher, J.C., Smith, D.C., Stephenson, N.C.N., Ungaretti, L., Whittaker, E.J.W., Youzhi, G., 1997, Nomenclature of amphiboles; Report of the Subcommittee on Amphiboles of the International Mineralogical Association, Commission on New Minerals and Mineral Names: American Mineralogist, 82(9-10), 1019-1037.

Manton, W.I., 1996, The Grenville of Honduras (abstract), *in* Geological Society of America Annual Meeting, Denver, Colorado: Geological Society of America, Abstracts with Programs, 28, A-493.

Martens, U., Ratschbacher, L., McWilliams, M., 2005, U-Pb Geochronology of the Maya Block, Guatemala (abstract): Eos Transactions, American Geophysical Union, 86(52), Fall Meeting Supplement, Abstract T51D-1387.

Martens, U., Weber, B., Valencia, V.A., 2006, Zircon geochronology implies the existence of pre-Devonian sedimentary rocks with

Grenvillian provenance in the Maya Mountains of Belize (abstract) *in*: Geological Society of America Annual Meeting, Philadelphia, Pennsylvania: Geological Society of America, Abstracts with Programs, 38(7), p. 504.

Martens, U., Liou, J.G., Solari, L.A., Mattison, C.G., Wooden, J., 2007, Petrotectonic evolution of the Chuacús Complex, central Guatemala, by U/Pb geochronology (abstract): Eos Transactions, American Geophysical Union, 88(52), Fall Meeting Supplement, Abstract T11D-08.

Morán-Centeno, D., 1984, Geología de la República Mexicana: México, Universidad Nacional Autónoma de México, Instituto Nacional de Estadística, Geografia e Informática (INEGI), 88 p.

Muehlberger, W.R., Ritchie, A.W., 1975, Caribbean-Americas plate boundary in Guatemala and southern Mexico as seen on *Skylab IV* orbital photography: Geology, 3(5), 232-235.

Nelson, B.K., Herrmann, U.R., Gordon, M.B., Ratschbacher, L., 1997, Sm-Nd and U-Pb evidence for Proterozoic crust for in the Chortis block, Central America: Comparison with the crustal history of southern Mexico: Terra Nova, 9(1), 496.

Ortega-Gutiérrez, F., 1981, Metamorphic belts of Southern Mexico and their tectonic significance: Geofísica Internacional, 20, 177-202.

Ortega-Gutiérrez, F., 1984, Evidence of Precambrian evaporites in the Oaxacan granulite complex of southern Mexico: Precambrian Research, 23, 377-393.

Ortega-Gutiérrez, F., Solari, L.A., Solé, J., Martens, U., Gómez-Tuena, A., Morán-Ical, S., Reyes-Salas, M., Ortega-Obregón, C., 2004, Polyphase, high-temperature eclogite-facies metamorphism in the Chuacús Complex, central Guatemala: Petrology, geochronology, and tectonic implications: International Geology Review, 46, 445-470.

Ortega-Gutiérrez, F., Solari, L.A., Ortega-Obregón, C., Elías-Herrera, M., Martens, U., Morán-Ical, S., Chiquín, M., Keppie, J.D., Torres de León, R., Schaaf, P., 2007, The Maya-Chortis boundary: a tectonostratigraphic approach: International Geology Review, 49(11), 996-1024.

Schaaf, P., Weber, B., Weis, P., Groβ, A., Ortega-Gutiérrez, F., Kohler, H., 2002, The Chiapas Massif (Mexico) revised: New geologic and isotopic data and basement characteristics, *in* Miller, H.E. (ed.), Contributions to Latin-American Geology: Neues Jahrbuch für Geologie und Paläontologie, Abhandlungen, 1-23.

Sedlock, R.L., Ortega-Gutiérrez, F., Speed, R.C., 1993, Tectonostratigraphic terranes and tectonic evolution of Mexico: Geological Society of America, Special Paper 278, 153.

Solari, L.A., Dostal, J., Ortega-Gutiérrez, F., Keppie, J.D., 2001, The 275 Ma arc-related La Carbonera Stock in the northern Oaxaca Complex of southern Mexico: U-Pb geochronology and geochemistry: Revista Mexicana de Ciencias Geológicas, 18(2), 149-161.

Solari, L.A., Keppie, J.D., Ortega-Gutiérrez, F., Cameron, K.L., Lopez, R., Hames, W.E., 2003, 990 and 1100 Ma Grenvillian tectonothermal events in the northern Oaxacan complex, southern México: roots of an orogen: Tectonophysics, 365, 257-282.

Solari, L.A., Ortega-Gutiérrez, F., Elías-Herrera, M., Schaaf, P., Norman, M., Torres de León, R., Ortega-Obregón, C., Chiquín, M., Morán-Ical, S., in press, U-Pb zircon geochronology of Paleozoic units in Western and Central Guatemala: insights into the tectonic evolution of Middle America, *in* Pindell, J., James, K.H. (ed.), Origin of the Caribbean Plate: Journal of the Geological Society of London, Special Publication.

Spear, F.S., Kohn, M.J., 1999, Program Thermobarometry [on-line] v. 2.1: Rensselaer Polytechnic Institute, Department of Earth & Environmental Sciences, Metamorphic Petrology Research Laboratory, <http://ees2.geo.rpi.edu/MetaPetaRen/Software/Software.html>.

Spear, F.S., Kohn, M.J., Florence, F.P., Menard, T., 1990, A model for garnet and plagioclase growth in pelitic schists: implications for thermobarometry and P-T path determinations: Journal of Metamorphic Geology, 8 (6), 683-696.

Steiner, M.B., Walker, J.D., 1996, Late Silurian plutons in Yucatan: Journal of Geophysical Research, 101(B8), 17727-17735.

Torres, R., Ruiz, J., Patchett, P.J., Grajales, J.M, 1999, Permo-Triassic continental arc in eastern Mexico: Tectonic implications for reconstructions of southern North America: Geological Society of America, Special Paper 340, 191–196.

Viele, G.W., Thomas, W.A., 1989, Tectonic synthesis of the Ouachita orogenic belt, *in* Hatcher, R.D. Jr., Thomas W.A., Viele, G.W. (eds.), The Apalachian-Ouachita Orogen in the United States: Boulder, Colorado, Geological Society of America, Geology of North America, F-2, 695-728.

Weber, B., Köhler, H., 1999, Sm-Nd, Rb-Sr and U-Pb isotope geochronology of a Grenville terrane in Southern México: Origin and geologic history of the Guichicovi complex: Precambrian Research, 96, 245-262.

Weber, B., López-Martínez, M., 2006, Pb, Sr, and Nd isotopic and chemical evidence for an oceanic island arc formation of the El Arco porphyry copper deposit (Baja California, Mexico): Mineralium Deposita, 40(6-7), 707-725.

Weber, B., Gruner, B., Hecht, L., Molina-Garza, R., Köhler, H., 2002, El descubrimiento de basamento metasedimentario en el macizo de Chiapas: La "Unidad La Sepultura": GEOS, 22(1), 2-11.

Weber, B., Cameron, K.L., Osorio, M., Schaaf, P., 2005, A late Permian tectonothermal event in Grenville crust of the Southern Maya terrane: U-Pb zircon ages from the Chiapas massif, Southeastern Mexico: International Geology Review, 47, 509-529.

Weber, B., Iriondo, A., Premo, W.R., Hecht, L., Schaaf, P., 2007, New insights into the history and origin of the southern Maya Block, SE México: U-Pb-SHRIMP zircon geochronology from metamorphic rocks of the Chiapas Massif: International Journal of Earth Sciences (Geologische Rundschau), 96, 253-269.

Weber, B., Valencia, V.A., Schaaf, P., Pompa Mera, V., Ruiz, J., 2008, Significance of provenance ages from the Chiapas Massif complex (SE México): Redefining the Paleozoic basement of the Maya block and its evolution in a Peri-Gondwanan realm: The Journal of Geology, 116(6), 619-637.

Yañez, P., Ruiz, J., Patchett,P.J., Ortega-Gutiérrez, F., Gehrels, G.E., 1991, Isotopic studies of the Acatlán Complex, southern Mexico: Implications for Paleozoic North American tectonics: Geological Society of America Bulletin, 103, 817-828.

Manuscript received: February 26, 2008
Corrected manuscript received: October 29, 2008
Manuscript aceppted: November 8, 2008